

Meshless Local Integral Equations Formulation for the 2D Convection-Diffusion Equations with a Nonlocal Boundary Condition

Ahmad Shirzadi ¹

Abstract: This paper presents a meshless method based on the meshless local integral equation (LIE) method for solving the two-dimensional diffusion and diffusion-convection equations subject to a non-local condition. Suitable finite difference scheme is used to eliminate the time dependence of the problem. A weak formulation on local subdomains with employing the fundamental solution of the Laplace equation as test function transforms the resultant elliptic type equations into local integral equations. Then, the Moving Least Squares (MLS) approximation is employed for discretizing spatial variables. Two illustrative examples with exact solutions being used as benchmark solutions are presented to show the efficiency of the proposed method.

Keywords: Meshless methods; Local integral equations; Nonlocal integral condition; Time dependent problems; Finite differences.

1 Introduction

The number of publications in the field of meshless methods reveals that these methods have become very popular in recent years. A relatively large number of the existing meshless methods are based on the use of strong form equation such as the meshless collocation method based on radial basis functions which was originated by Kansa [Kansa (1986)]. Focusing on the points and using strong form equation make these kinds of methods unstable and special attention is needed in choosing points [Ling and Schaback (2008); Ling and Hon (2005)]. In the meshless methods which use the weak form equation such as the element free Galerkin (EFG) method [Belytschko, Lu, and Gu (1994); Zhang, Liew, Cheng, and Lee (2008)] the evaluation of integrals on the whole domain is necessary. However, subject to precise evaluation of integrals, the results are of high accuracy and stabil-

¹ Department of Mathematics, Persian Gulf University, Bushehr, Iran, email: shirzadi@pgu.ac.ir, shirzadi.a@gmail.com

ity. The meshless local Petrov-Galerkin (MLPG) method [Atluri and Zhu (1998a); Atluri and Zhu (1998b); Atluri (2004); Atluri and Shen (2002)] and the meshless LIE method [Sladek, Sladek, and Atluri (2000); Zhu, Zhang, and Atluri (1998); Long and Zhang (2002); Tulong, Jindong, and Atluri (1999)] have the advantage of easy implementation, stability and accuracy, because the method uses the *weak* form equation on the local nodal based *subdomains*. These methods have been successfully applied in various branches of science and engineering, [Ching and Batra (2001); Qian, Batra, and Chen (2004); Mirzaei and Dehghan (2010); Sellountos, Sequeira, and Polyzos (2011); Dehghan and Mirzaei (2009); Shirzadi, Ling, and Abbasbandy (2012)] being among them.

In the mathematical modeling of various processes, an integral term appears over the spatial domain or in the boundary conditions. Such problems are known as non-local problems. For some application of these kinds of problems see [Cannon and van der Hoek (1986); Cannon and Lin (1990); Capasso and Kunisch (1988)]. There exist also many paper investigating the numerical solutions of these kind of problems, for example see [Abbasbandy and Shirzadi (2010); Abbasbandy and Shirzadi (2011)] for MLPG formulation, [Ang (2001)] for boundary integral equation method, [Dehghan (2002)] for finite differences, [Dehghan and ShamSi (2006)] for pseudospectral Legendre method and many others [Ang (2008); Dehghan (2005a); Noye and Dehghan (1994); Dehghan (2003); Dehghan (2006); Dehghan (2007); Dehghan (2005b)]. The purpose of this article is to present a meshless method for solution of following two-dimensional diffusion and convection-diffusion equations in two spatial dimensions:

$$\frac{\partial u(x,y,t)}{\partial t} = \nabla^2 u(x,y,t) + \omega \cdot \nabla u(x,y,t) + f(x,y,t) \quad (1)$$

with initial and boundary conditions:

$$u(x,y,0) = u_0(x,y), \quad 0 \leq x,y \leq 1, \quad (2)$$

$$\frac{\partial u(x,y,t)}{\partial x} \Big|_{x=0} = g_0(y,t), \quad 0 \leq t \leq T, \quad 0 \leq y \leq 1, \quad (3)$$

$$\frac{\partial u(x,y,t)}{\partial x} \Big|_{x=1} = g_1(y,t), \quad 0 \leq t \leq T, \quad 0 \leq y \leq 1, \quad (4)$$

$$u(x,1,t) = h_1(x,t), \quad 0 \leq t \leq T, \quad 0 \leq x \leq 1, \quad (5)$$

$$u(x,0,t) = h_0(x)\mu(t), \quad 0 \leq t \leq T, \quad 0 \leq x \leq 1, \quad (6)$$

and the nonlocal boundary condition

$$\int_0^1 \int_0^1 u(x,y,t) dx dy = m(t), \quad 0 \leq x \leq 1, \quad (7)$$

where f , u_0 , g_0 , g_1 , h_0 , h_1 and m are known functions, while the functions u and μ are unknown. $\omega = (\omega_1, \omega_2)$ is the convection coefficient. The boundary condition (Eq. 6) is variable separable, with spatial dependence given by $h_0(x)$ and time dependence given by $\mu(t)$.

The presented method in this paper eliminates the time dependence of the problem by using a finite difference scheme. Then, the original parabolic PDE is converted into elliptic ones for the field variables at discrete time instants. A weak formulation on local subdomains with employing the fundamental solution of the Laplace equation as test function transforms the elliptic PDEs into local integral equations. The MLS approximation is employed for spatial variations of the field variables at discrete time instants. In the case of using a fundamental solution as test function, it is important that how evaluate the integrals. For evaluating the regular local boundary integrals Gauss-Legendre quadrature rule is used in this paper and certain approximations are presented for the evaluation of the domain and singular integrals occurring in the weak formulation. As first test example the governing equations are given by diffusion equation and the last test problem is a convection-diffusion equations.

2 Finite difference approximations

Suppose the time interval $[0, T]$ is discretized uniformly into K subintervals; define $t_k = k\Delta t$, $k = 0, 1, \dots, K$, where $\Delta t = T/K$ is the time step. Let $u^k = u^k(\mathbf{x}) := u(\mathbf{x}, t_k)$ be the exact solution u restricted to time t_k . Then, the finite-difference approximation of the time derivatives in the θ method is given as follows

$$\theta \dot{u}^{k+1} + (1 - \theta) \dot{u}^k = \frac{u^{k+1} - u^k}{\Delta t} + O(\Delta t), \quad 0 \leq \theta \leq 1. \quad (8)$$

Considering (Eq. 1) at the time instants $k\Delta t$ and $(k+1)\Delta t$, one obtains, respectively

$$\begin{aligned} (1 - \theta) \theta \dot{u}^k &= (1 - \theta) \nabla^2 u^k + (1 - \theta) \omega \cdot \nabla u^k + (1 - \theta) f(x, y, k\Delta t), \\ \theta \dot{u}^{k+1} &= \theta \nabla^2 u^{k+1} + \theta \omega \cdot \nabla u^{k+1} + \theta f(x, y, (k+1)\Delta t), \end{aligned}$$

Hence and from (Eq. 8), we have

$$\begin{aligned} \frac{u^{k+1} - u^k}{\Delta t} &= \nabla^2 u^k + \theta \left(\nabla^2 u^{k+1} - \nabla^2 u^k \right) + \omega \cdot \nabla u^k \\ &+ \theta \left(\omega \cdot \nabla u^{k+1} - \omega \cdot \nabla u^k \right) + \theta f(x, y, (k+1)\Delta t) \\ &+ (1 - \theta) f(x, y, k\Delta t). \end{aligned} \quad (9)$$

In this paper the Crank-Nicholson scheme, $\theta = \frac{1}{2}$, is used and therefore (Eq. 9) becomes:

$$\frac{u^{k+1} - u^k}{\Delta t} = \frac{1}{2} (\nabla^2 + \omega \cdot \nabla) (u^{k+1} + u^k) + \frac{1}{2} (f^{k+1} + f^k),$$

or

$$\begin{aligned} \left(1 - \frac{\Delta t}{2} (\nabla^2 + \omega \cdot \nabla)\right) u^{k+1} &= \left(1 + \frac{\Delta t}{2} (\nabla^2 + \omega \cdot \nabla)\right) u^k \\ &+ \frac{\Delta t}{2} (f^{k+1} + f^k). \end{aligned} \quad (10)$$

So, assuming the field u^k being known from the computation in the previous time step, the field variable u^{k+1} can be obtained via elliptic type PDE (Eq. 10).

To treat the Neumann's boundary conditions, we use the following finite difference schemes which are of order $O(h^3)$

$$\left. \frac{\partial u^k(x, y)}{\partial x} \right|_{x=0} = \frac{1}{h} \left(-\frac{11}{6} u^k(0, y) + 3u^k(h, y) - \frac{3}{2} u^k(2h, y) + \frac{1}{3} u^k(3h, y) \right), \quad (11)$$

$$\begin{aligned} \left. \frac{\partial u^k(x, y)}{\partial x} \right|_{x=1} &= \frac{1}{h} \left(\frac{11}{6} u^k(1, y) - 3u^k(1-h, y) + \frac{3}{2} u^k(1-2h, y) \right. \\ &\left. - \frac{1}{3} u^k(1-3h, y) \right). \end{aligned} \quad (12)$$

Finite differences approximation to impose Neumann's boundary condition in the MLPG method is used in [Abbasbandy and Shirzadi (2011)].

3 Local integral formulation

we construct a local weak form of (Eq. 10) over some sub-domains Ω_s . These sub-domains could be of any geometric shape and size in the global domain Ω . In this paper, we use sub-domains of circular shape with radius r_0 centered at node $\mathbf{x}^i = (x^i, y^i) \in \Omega_s^i \subset \Omega$. The local weak form of (Eq. 10) over Ω_s^i is:

$$\begin{aligned} \int_{\Omega_s^i} \left[\left(1 - \frac{\Delta t}{2} (\nabla^2 + \omega \cdot \nabla)\right) u^{k+1} \right] v d\mathbf{x} &= \\ \int_{\Omega_s^i} \left[\left(1 + \frac{\Delta t}{2} (\nabla^2 + \omega \cdot \nabla)\right) u^k + \frac{\Delta t}{2} (f^{k+1} + f^k) \right] v d\mathbf{x}. \end{aligned} \quad (13)$$

It is well known that $u^* = -\frac{1}{2\pi} \ln(r) + C$ is a fundamental solution corresponding to the poisson's equation, i.e., $\nabla^2 u^* + \delta(x, y) = 0$, where C is an arbitrary constant,

$\delta(x, y)$ is the Dirac delta function and r is the distance between the field and source points, i.e., $r = \|\mathbf{x} - \mathbf{x}^i\|$. If we choose $C = \frac{1}{2\pi}Ln(r_0)$ where r_0 is the radius of the circular sub-domain Ω_s^i centered at point \mathbf{x}^i then the modified fundamental solution to the poisson's equation can be given by

$$u^* = -\frac{1}{2\pi}Ln\left(\frac{r}{r_0}\right).$$

If u^* is chosen as the test function in each sub-domain, then using the divergence theorem and since u^* vanishes on $\partial\Omega_s^i$, the local weak form equation can be transformed into the following simple local integral equation

$$\begin{aligned} & \int_{\Omega_s^i} u^{k+1} u^* d\mathbf{x} + \frac{\Delta t}{2} \left(u^{k+1}(\mathbf{x}^i) + \int_{\partial\Omega_s^i} u^{k+1} \frac{\partial u^*}{\partial n} ds \right) \\ & - \frac{\Delta t}{2} \int_{\Omega_s^i} \boldsymbol{\omega} \cdot \nabla u^{k+1} u^* d\mathbf{x} = \int_{\Omega_s^i} u^k u^* d\mathbf{x} \\ & - \frac{\Delta t}{2} \left(u^k(\mathbf{x}^i) + \int_{\partial\Omega_s^i} u^k \frac{\partial u^*}{\partial n} ds \right) + \frac{\Delta t}{2} \int_{\Omega_s^i} \boldsymbol{\omega} \cdot \nabla u^k u^* d\mathbf{x} \\ & + \frac{\Delta t}{2} \int_{\Omega_s^i} u^* (f^{k+1} + f^k) d\mathbf{x} \end{aligned} \quad (14)$$

where $\partial\Omega_s^i$ is the boundary of Ω_s^i , $n = (n_1, n_2)$ is the outward unit normal to the boundary $\partial\Omega_s^i$, and $\frac{\partial u}{\partial n}$ is the normal derivative.

4 Spatial discretizations and implementation

The moving least-squares (MLS) approximation is employed to form the trial space in this work. The MLS polynomial basis represents the trial function with the fictitious values of the unknown function at N given nodes $\Xi := \{\mathbf{x}_1, \dots, \mathbf{x}_N\}$. Let $\mathbf{p}^T(\mathbf{x}) = [p_1(\mathbf{x}), p_2(\mathbf{x}), \dots, p_m(\mathbf{x})]$ be a complete monomial basis of (pre-defined) order m ; for example, for 2D problems with $\mathbf{x} = (x, y)$, it could be $\mathbf{p}^T(\mathbf{x}) = [1, x, y]$ or $\mathbf{p}^T(\mathbf{x}) = [1, x, y, x^2, xy, y^2]$, for linear basis ($m = 3$) and quadratic basis ($m = 6$), respectively. We allow the vector function \mathbf{p}^T to take the set of points as input and return a matrix of size $(\# \text{ points}) \times m$. In particular, we denote the $N \times m$ matrix $P = \mathbf{p}^T(\Xi)$ with entries $[P_{ij}] = p_j(\mathbf{x}_i)$ for $i = 1, \dots, N$, $j = 1, \dots, m$, and $\mathbf{x}_i \in \Xi$. Also at each node \mathbf{x}_i , a compactly supported weight function $w_i > 0$ is assigned. In this work, the Gaussian weight function is used

$$w_i(\mathbf{x}) = \begin{cases} \frac{e^{[-(\|\mathbf{x} - \mathbf{x}_i\|/c_i)^2]} - e^{[-(r_i/c_i)^2]}}{1 - e^{[-(r_i/c_i)^2]}}, & 0 \leq \|\mathbf{x} - \mathbf{x}_i\| < r_i, \\ 0, & \text{otherwise,} \end{cases} \quad (15)$$

where $c_i > 0$ is a constant controlling the shape of the weight function w_i , and $r_i > 0$ determines the support size. Note that in this paper c_i and r_i are fixed with $c_i = c$ and $r_i = R$ for all nodes, but they can be made node-dependent for higher flexibility. We construct a MLS polynomial basis for the distribution of a function u at Ξ as follows. We seek a MLS approximation U in the form of

$$U(\mathbf{x}) = \mathbf{p}^T(\mathbf{x})\mathbf{a}(\mathbf{x}) \quad (16)$$

in which the (moving) coefficient vector $\mathbf{a}(\mathbf{x}) = [a_1(\mathbf{x}), \dots, a_m(\mathbf{x})]$ at each \mathbf{x} is determined by minimizing a weighted discrete L_2 -norm residual functional at the N nodal values

$$J(\mathbf{a})(\mathbf{x}) = \sum_{\mathbf{x}_i \in \Xi} w_i(\mathbf{x}) (\mathbf{p}^T(\mathbf{x}_i)\mathbf{a}(\mathbf{x}) - u(\mathbf{x}_i))^2. \quad (17)$$

Solving (Eq. 17) from a small-scale linear system yields

$$\mathbf{a}(\mathbf{x}) = (P^T W(\mathbf{x}) P)^{-1} P^T W(\mathbf{x}) u(\Xi) \quad (18)$$

where the vector is $u(\Xi)^T = [u(\mathbf{x}_1), \dots, u(\mathbf{x}_N)]$, and the matrix function is defined as $W(\mathbf{x}) = \text{diag}(w_1(\mathbf{x}), \dots, w_N(\mathbf{x}))$. From another point of view, the trial function implicitly defined by (Eq. 16) and (Eq. 18) can be rewritten as

$$U(\mathbf{x}) = \underbrace{\mathbf{p}^T(\mathbf{x}) (P^T W(\mathbf{x}) P)^{-1} P^T W(\mathbf{x})}_{\Phi(\mathbf{x})} u(\Xi) = \sum_{i=1}^N u(\mathbf{x}_i) \phi_i(\mathbf{x}), \quad (19)$$

where trial basis (or shape function) ϕ_i is the i -th entry in the vector function $\Phi : \mathbb{R}^2 \rightarrow \mathbb{R}^{1 \times N}$. Unless u is a polynomial of degree less than or equal to m , we see that the MLS approximation $U(\mathbf{x}_i) \approx u(\mathbf{x}_i)$ but $U(\mathbf{x}_i) \neq u(\mathbf{x}_i)$ for $\mathbf{x}_i \in \Xi$ as seen in quasi-interpolation schemes. Differentiating the MLS basis ϕ_i requires derivatives of the weight functions and that of some low-order polynomials only. Expanding u^k by (Eq. 19) results in

$$u(\mathbf{x}, t_k) = u^k(\mathbf{x}) \approx \sum_{j=1}^N U_j^k \phi_j(\mathbf{x}).$$

and from the weak formulation (Eq. 14), yields in each sub-domain Ω_s^i

$$\begin{aligned}
& \sum_{j=1}^N \left(\int_{\Omega_s^i} \phi_j u^* d\mathbf{x} \right) U_j^{k+1} + \frac{\Delta t}{2} \sum_{j=1}^N \left(\phi_j(\mathbf{x}^i) + \int_{\partial\Omega_s^i} \phi_j \frac{\partial u^*}{\partial n} ds \right) U_j^{k+1} \\
& - \frac{\Delta t}{2} \sum_{j=1}^N \left(\int_{\Omega_s^i} (\boldsymbol{\omega} \cdot \nabla \phi_j) u^* d\mathbf{x} \right) U_j^{k+1} = \\
& \sum_{j=1}^N \left(\int_{\Omega_s^i} \phi_j u^* d\mathbf{x} \right) U_j^k - \frac{\Delta t}{2} \sum_{j=1}^N \left(\phi_j(\mathbf{x}^i) + \int_{\partial\Omega_s^i} \phi_j \frac{\partial u^*}{\partial n} ds \right) U_j^k \\
& + \frac{\Delta t}{2} \sum_{j=1}^N \left(\int_{\Omega_s^i} (\boldsymbol{\omega} \cdot \nabla \phi_j) u^* d\mathbf{x} \right) U_j^{k+1} + \frac{\Delta t}{2} \int_{\Omega_s^i} u^* (f^{k+1} + f^k) d\mathbf{x}
\end{aligned} \tag{20}$$

To impose the boundary conditions using the boundary nodes, we adopt our proposed method in [Abbasbandy and Shirzadi (2011)] which for the ease of reader is represented as follows:

For nodes $\mathbf{x}^l = (0, y^l)$ on the left vertical boundary ($0 \leq y^l \leq 1$), using (11) and the MLS approximation, we have

$$\begin{aligned}
& \frac{\partial u^{k+1}(\mathbf{x}^l)}{\partial x} \approx \\
& \frac{1}{h} \left(-\frac{11}{6} \sum_{i=1}^{n^l} \phi_i(\mathbf{x}^l) U_i^{k+1} + 3 \sum_{i=1}^{n^{l+1}} \phi_i(\mathbf{x}^{l+1}) U_i^{k+1} - \frac{3}{2} \sum_{i=1}^{n^{l+2}} \phi_i(\mathbf{x}^{l+2}) U_i^{k+1} + \right. \\
& \left. \frac{1}{3} \sum_{i=1}^{n^{l+3}} \phi_i(\mathbf{x}^{l+3}) U_i^{k+1} \right) + O(h^3) = g_0(\mathbf{x}^l, (k+1)\Delta t).
\end{aligned} \tag{21}$$

with $\mathbf{x}^{l+a} = (ah, y^l)$

For nodes $\mathbf{x}^l = (1, y^l)$ on the right vertical boundary ($0 \leq y^l \leq 1$), using (12) and the MLS approximation, we have

$$\begin{aligned}
& \frac{\partial u^{k+1}(\mathbf{x}^l)}{\partial x} \approx \\
& \frac{1}{h} \left(\frac{11}{6} \sum_{i=1}^{n^l} \phi_i(\mathbf{x}^l) U_i^{k+1} - 3 \sum_{i=1}^{n^{l-1}} \phi_i(\mathbf{x}^{l-1}) U_i^{k+1} + \frac{3}{2} \sum_{i=1}^{n^{l-2}} \phi_i(\mathbf{x}^{l-2}) U_i^{k+1} + \right. \\
& \left. - \frac{1}{3} \sum_{i=1}^{n^{l-3}} \phi_i(\mathbf{x}^{l-3}) U_i^{k+1} \right) + O(h^3) = g_1(\mathbf{x}^l, (k+1)\Delta t).
\end{aligned} \tag{22}$$

with $\mathbf{x}^{l-a} = (1 - ah, y^l)$

For nodes $\mathbf{x}^l = (x^l, 1)$ on the top horizontal boundary ($0 \leq x^l \leq 1$), using (5) and the MLS approximation, we have

$$\sum_{i=1}^{n^l} \phi_i(\mathbf{x}^l) U_i^{k+1} = h_1(\mathbf{x}^l, (k+1)\Delta t). \quad (23)$$

For nodes $\mathbf{x}^l = (x^l, 0)$ on the bottom horizontal boundary ($0 \leq x^l \leq 1$), using (6) we have

$$\sum_{i=1}^{n^l} \phi_i(\mathbf{x}^l) U_i^{k+1} - h_0(\mathbf{x}^l) \hat{\mu}^{k+1} = 0. \quad (24)$$

Using Simpson's composite numerical integration rule and the MLS approximation, the double integral in (7) is approximated in the following way:

$$\begin{aligned} \int_0^1 \int_0^1 u^{k+1}(x, y) dx dy &\approx \sum_{j=1}^N d_j u_j^{k+1} = \sum_{j=1}^N d_j \sum_{i=1}^n \phi_i(\mathbf{x}^j) U_i^{k+1} \\ &= \sum_{i=1}^N \left(\sum_{j=1}^n d_j \phi_i(\mathbf{x}^j) \right) U_i^{k+1} = m((k+1)\Delta t), \end{aligned} \quad (25)$$

where d_j 's are Simpson's composite numerical integration rule coefficients. Equations 20-25 define $N + 1$ linear equations which can be solved for the $N + 1$ unknowns U and μ .

5 Evaluation of integrals

For the regular local boundary integrals eight points Gauss-Legendre quadrature rule is used as follows:

$$\begin{aligned} &\int_{\partial\Omega_i^*} \phi_j(\mathbf{x}) \frac{\partial u^*}{\partial n}(\mathbf{x}, \mathbf{x}^i) ds \\ &= \int_0^{2\pi} \frac{-1}{2\pi r_0} \phi_j(x^i + r_0 \cos(\theta), y^i + r_0 \sin(\theta)) r_0 d\theta \\ &= -\frac{1}{2} \int_{-1}^1 \phi_j(x^i + r_0 \cos(\pi\theta + \pi), y^i + r_0 \sin(\pi\theta + \pi)) d\theta \\ &\approx -\frac{1}{2} \sum_{p=1}^8 w_p \phi_j(x^i + r_0 \cos(\pi\theta_p + \pi), y^i + r_0 \sin(\pi\theta_p + \pi)) \end{aligned}$$

where w_p and θ_p are the Gauss quadrature integration rule weights and points on $[-1, 1]$, respectively. The local domain integrals for test function can be obtained analytically as follows:

$$\int_{\Omega_s^i} u^*(\mathbf{x}, \mathbf{x}^i) d\mathbf{x} = - \int_0^{2\pi} \int_0^{r_0} \frac{r}{2\pi} \ln \frac{r}{r_0} dr d\theta = \frac{1}{4} r_0^2,$$

so, we use the following approximations:

$$\begin{aligned} & \int_{\Omega_s^i} u^*(\mathbf{x}, \mathbf{x}^i) \frac{\partial \phi_j(\mathbf{x})}{\partial x} d\mathbf{x} \\ & \approx \frac{\partial \phi_j(\mathbf{x})}{\partial x} \Big|_{\mathbf{x}=\mathbf{x}^i} \int_{\Omega_s^i} u^*(\mathbf{x}, \mathbf{x}^i) d\mathbf{x} = \frac{1}{4} \frac{\partial \phi_j(\mathbf{x})}{\partial x} \Big|_{\mathbf{x}=\mathbf{x}^i} r_0^2, \end{aligned}$$

and similarly

$$\int_{\Omega_s^i} u^*(\mathbf{x}, \mathbf{x}^i) \phi_j(\mathbf{x}) d\mathbf{x} \approx \phi_j(\mathbf{x}^i) \int_{\Omega_s^i} u^*(\mathbf{x}, \mathbf{x}^i) d\mathbf{x} = \frac{1}{4} \phi_j(\mathbf{x}^i) r_0^2.$$

Precise evaluating the local integrals will increase the computational efficiency of local integral equation method [Sladek and Sladek (2010); Sladek, Sladek, and Zhang (2010)]. We refer the interested reader to [Mazzia, Ferronato, Pini, and Gambolati (2007)] for quadrature rule for MLPG.

6 Numerical demonstration

Recall that r_0 is the radius of each local sub-domains and r_i is the radius of the support of the weight function corresponding to node i . For the MLS approximations, the quadratic basis is used in this paper. The gaussian weight function is used for the MLS approximation and $c_i \approx h$, where h is the distance between two consecutive nodes in each direction. The distribution of nodes are regular in the examples. Because of the computational techniques described in the previous section, r_0 should be small enough. A very small r_0 also causes much cancelation error. So it is chosen as $r_0 \approx 0.05h$ in this paper. For the MLS moment matrix to be invertible, the support of weight functions, r_i , should be large enough to have sufficient number of nodes covered in the domain of definition of every sample point. On the other hand, it should be small enough to preserve the local character of the approximation. In this paper it is chosen as $r_i \approx 3h$. In this work, the infinity norm error which will be reported is defined as:

$$\begin{aligned} \|e_u\|_\infty &= \text{Max}\{|u_i - \bar{u}_i|, \quad i = 1, 2, \dots, M\}, \\ \|e_\mu\|_\infty &= |\mu - \bar{\mu}|, \end{aligned}$$

and the relative error is defined as:

$$\|e_u\|_R = \sqrt{\frac{\sum_{i=1}^M (u_i - \bar{u}_i)^2}{\sum_{i=1}^M u_i^2}},$$

$$\|e_\mu\|_R = \frac{\mu - \bar{\mu}}{\mu},$$

where $\bar{\mu}$ is the numerical approximation of μ , \bar{u}_i is the numerical approximation of u at node i , and errors are computed in M number of nodes for which in general M is greater than N .

6.1 Test Problem 1.

Consider the diffusion equation:

$$\frac{\partial u(x, y, t)}{\partial t} = \nabla^2 u(x, y, t)$$

with conditions:

$$u(x, y, 0) = \exp(x + y), \quad 0 \leq x, y \leq 1,$$

$$\left. \frac{\partial u(x, y, t)}{\partial x} \right|_{x=0} = \exp(y + 2t), \quad 0 \leq t \leq T, \quad 0 \leq y \leq 1,$$

$$\left. \frac{\partial u(x, y, t)}{\partial x} \right|_{x=1} = \exp(1 + y + 2t), \quad 0 \leq t \leq T, \quad 0 \leq y \leq 1,$$

$$u(x, 1, t) = \exp(1 + x + 2t), \quad 0 \leq t \leq T, \quad 0 \leq x \leq 1,$$

$$u(x, 0, t) = \exp(x)\mu(t), \quad 0 \leq t \leq T, \quad 0 \leq x \leq 1,$$

$$\int_0^1 \int_0^1 u(x, y, t) dx dy = \exp(2t) (\exp(2) - 2\exp(1) + 1),$$

for which the exact solution is

$$u(x, y, t) = \exp(x + y + 2t), \quad \mu(t) = \exp(2t).$$

Tab. 1 presents the results obtained at different time instants with $N = 441$ nodal points and time step $\Delta t = 0.001$. The results reveal that the proposed difference scheme is stable. The obtained results at time instant $t = 1$, with $N = 441$ nodal points and various Δt are presented in Tab. 2. By going through each column of Tab. 2 one can see increasing accuracy by decreasing the size of time step.

Fig. 1 presents the exact and approximate solution obtained for μ and Fig. 2 presents the approximate solution for u at time instant $t = 2.0$ with representation of error distribution. Both figures are obtained with using $N = 441$ nodal points and $\Delta t = 0.001$.

Table 1: The results obtained for example 1 at different time instants by using $N = 441$ nodal points and $\Delta t = 0.001$.

| t | μ | $\hat{\mu}$ | $\ e_\mu\ _R$ | $\ e_u\ _R$ |
|-----|-----------|-------------|---------------------------|---------------------------|
| 0.2 | 1.491825 | 1.491628 | 1.319581×10^{-4} | 8.449680×10^{-5} |
| 0.4 | 2.225541 | 2.225247 | 1.319734×10^{-4} | 8.524969×10^{-5} |
| 0.6 | 3.320117 | 3.319679 | 1.319734×10^{-4} | 8.525930×10^{-5} |
| 0.8 | 4.953032 | 4.952379 | 1.319733×10^{-4} | 8.525943×10^{-5} |
| 1.0 | 7.389056 | 7.388081 | 1.319733×10^{-4} | 8.525942×10^{-5} |
| 1.2 | 11.023176 | 11.021722 | 1.319734×10^{-4} | 8.525943×10^{-5} |
| 2.0 | 54.598150 | 54.590945 | 1.319734×10^{-4} | 8.525940×10^{-5} |

Table 2: The results obtained at time instant $t = 1$ by using $N = 441$ nodal points and different Δt for example 1.

| Δt | $\ e_\mu\ _R$ | $\ e_u\ _R$ |
|------------|---------------------------|---------------------------|
| 0.1 | 1.897967×10^{-3} | 4.409193×10^{-4} |
| 0.05 | 5.797418×10^{-4} | 1.570939×10^{-4} |
| 0.01 | 1.499823×10^{-4} | 8.707288×10^{-5} |
| 0.005 | 1.363395×10^{-4} | 8.568575×10^{-5} |
| 0.001 | 1.319733×10^{-4} | 8.525943×10^{-5} |

6.2 Test Problem 2.

Consider the following diffusion-convection equation

$$\frac{\partial u(x, y, t)}{\partial t} = \nabla^2 u(x, y, t) + \frac{\partial u(x, y, t)}{\partial x} - 2 \exp(x - y + t)$$

with conditions:

$$\begin{aligned}
 u(x, y, 0) &= \exp(x - y), \quad 0 \leq x, y \leq 1, \\
 \int_0^1 \int_0^1 u(x, y, t) dx dy &= \exp(t) (\exp(1) + \exp(-1) - 2), \\
 \frac{\partial u(x, y, t)}{\partial x} \Big|_{x=0} &= \exp(-y + t), \quad 0 \leq t \leq T, \quad 0 \leq y \leq 1, \\
 \frac{\partial u(x, y, t)}{\partial x} \Big|_{x=1} &= \exp(1 - y + t), \quad 0 \leq t \leq T, \quad 0 \leq y \leq 1, \\
 u(x, 1, t) &= \exp(x - 1 + t), \quad 0 \leq t \leq T, \quad 0 \leq x \leq 1, \\
 u(x, 0, t) &= \exp(x) \mu(t), \quad 0 \leq t \leq T, \quad 0 \leq x \leq 1,
 \end{aligned}$$

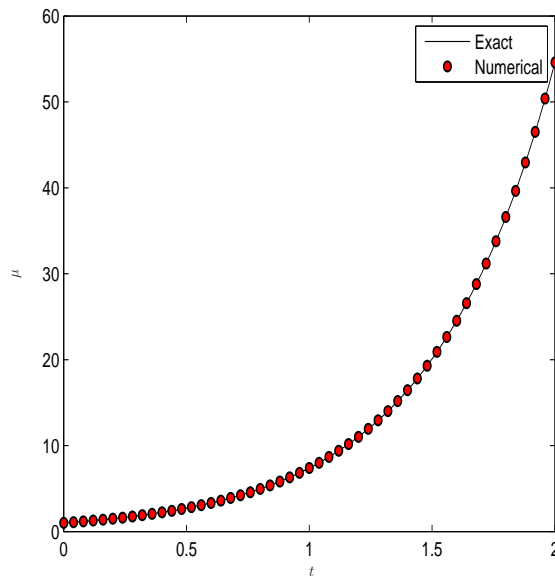


Figure 1: Exact and approximate solutions of μ with using $N=441$ nodal points and $\Delta t = 0.001$ for Example 1.

for which the exact solution is

$$u(x,y,t) = \exp(x - y + t), \quad \mu(t) = \exp(t).$$

Tab. 3 presents the results at different time instants for test problem 2 by using $N = 441$ nodal points and time step $\Delta t = 0.001$. The obtained results at time instant $t = 1$, with $N = 441$ nodal points and various Δt are presented in Tab. 4. Again the stability of the difference scheme is confirmed by considering these two tables.

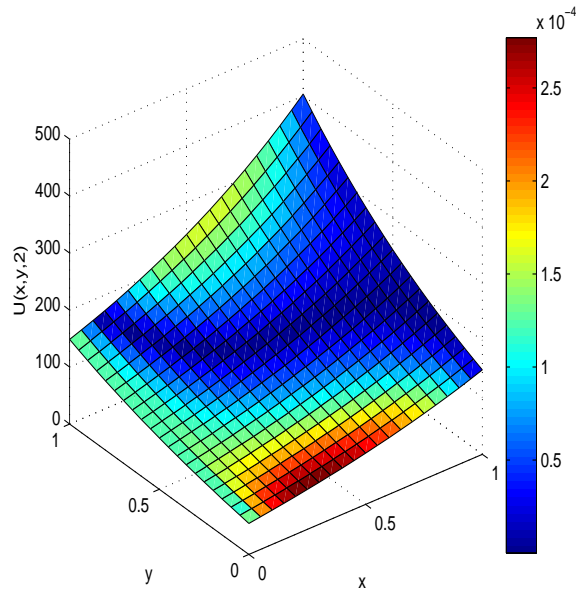


Figure 2: Numerical approximation of u at $t = 2.0$ with representation of error distribution(infinity norm error) obtained by using $N=441$ nodal points and $\Delta t = 0.001$ for Example 1.

In order to show the spatial convergence of the proposed method, we present Tab. 5. By going through each column of this table, increasing accuracy by increasing the number of nodal points can be seen.

Fig. 3 presents the exact and approximate solutions obtained for μ and Fig. 4 presents the approximate solution for u at time instant $t = 3.0$ with representation of error distribution. Both figures are obtained with $N = 441$ nodal points and

Table 3: The results obtained for example 2 at different time instants with using $\Delta t = 0.001$ and $N = 441$ nodal points.

| t | μ | $\hat{\mu}$ | $\ e_\mu\ _R$ | $\ e_u\ _R$ |
|-----|----------|-------------|---------------------------|---------------------------|
| 0.2 | 1.221402 | 1.221285 | 9.574279×10^{-5} | 9.558169×10^{-5} |
| 0.4 | 1.491824 | 1.491680 | 9.635099×10^{-5} | 9.656620×10^{-5} |
| 0.6 | 1.822118 | 1.821943 | 9.635809×10^{-5} | 9.657775×10^{-5} |
| 0.8 | 2.225540 | 2.225326 | 9.635817×10^{-5} | 9.657789×10^{-5} |
| 1.0 | 2.718281 | 2.718019 | 9.635817×10^{-5} | 9.657788×10^{-5} |
| 1.2 | 3.320116 | 3.319797 | 9.635817×10^{-5} | 9.657789×10^{-5} |
| 2.0 | 7.389056 | 7.388344 | 9.635817×10^{-5} | 9.657788×10^{-5} |

Table 4: The results obtained at time instant $t = 1$ by using $N = 441$ nodal points and different Δt for Example 2.

| Δt | $\ e_\mu\ _R$ | $\ e_u\ _R$ |
|------------|---------------------------|---------------------------|
| 0.1 | 1.703197×10^{-4} | 1.257931×10^{-4} |
| 0.05 | 1.143504×10^{-4} | 1.027325×10^{-4} |
| 0.01 | 9.720470×10^{-5} | 9.681802×10^{-5} |
| 0.005 | 9.656348×10^{-5} | 9.663597×10^{-5} |
| 0.001 | 9.635817×10^{-5} | 9.657788×10^{-5} |

Table 5: The results obtained at time instant $t = 1$ by using $\Delta t = 0.001$ and different number of nodal points for example 2.

| N | e_μ | $\ e_\mu\ _\infty$ | $\ e_u\ _R$ | $\ e_u\ _\infty$ |
|-----|---------------------------|---------------------------|---------------------------|---------------------------|
| 81 | 5.807570×10^{-4} | 1.578661×10^{-3} | 3.552693×10^{-4} | 4.291264×10^{-3} |
| 121 | 4.234847×10^{-4} | 1.151150×10^{-3} | 3.112411×10^{-4} | 3.603712×10^{-3} |
| 289 | 1.554610×10^{-4} | 4.225868×10^{-4} | 1.517228×10^{-4} | 1.279221×10^{-3} |
| 441 | 9.635817×10^{-5} | 2.619286×10^{-4} | 9.657788×10^{-5} | 8.404393×10^{-4} |

$\Delta t = 0.001$.

7 Conclusions

In the present paper, a meshless LIE method was proposed for numerical simulations of the two-dimensional diffusion and diffusion-convection equations subject to a non-local integral condition. A time stepping scheme was employed to approximate the time variable and its derivative. The fundamental solution of Laplace's equation was used as the test function in the local weak forms. The MLS ap-

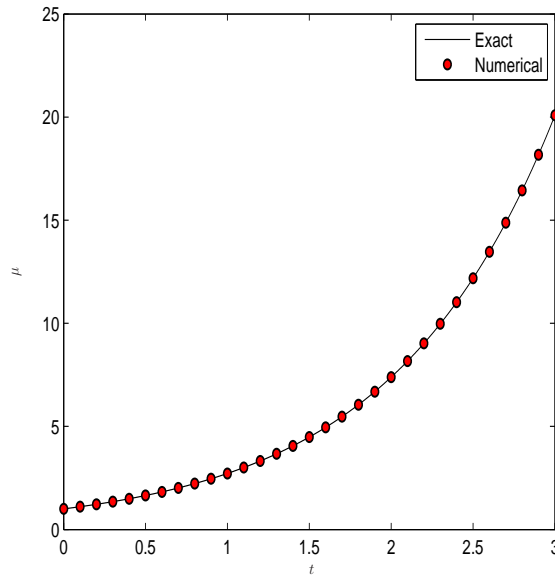


Figure 3: Exact and approximate solutions of μ with using $N=441$ nodal points and $\Delta t = 0.001$ for Example 2.

proximation was proposed to discretize the spatial variables. Collocation and finite difference approximations were used to impose the Dirichlet and Neumann's boundary conditions, respectively and the Simpson's composite numerical integration rule was suggested for discretizing the nonlocal integral condition. The method was successfully employed to numerically solve the nonlocal diffusion and diffusion convection equations with an integral condition. The results were confirming the stability and high accuracy of the method and the method can be applied to

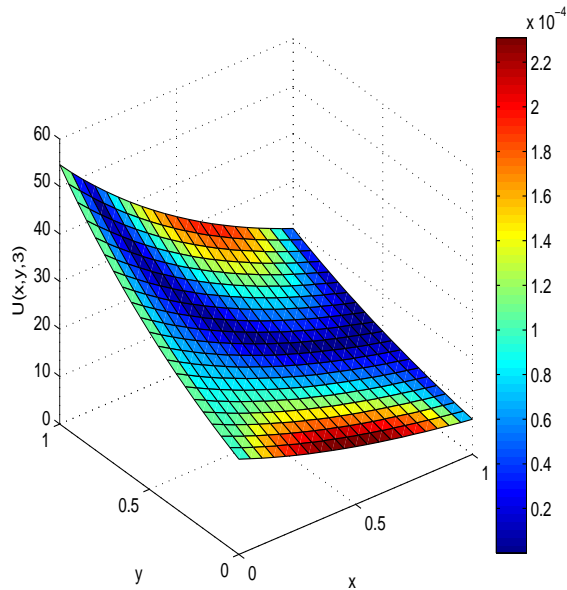


Figure 4: Approximate solutions for u at $t = 3.0$ with representation of error distribution(infinity norm error) by using $N=441$ nodal points and $\Delta t = 0.001$ for Example 2.

solve similar problems in engineering and sciences.

Acknowledgement: Financial support by the research committee of Persian Gulf University under project number PGU/SF/50-1/1390/1542 is greatly acknowledged.

References

- Abbasbandy, S.; Shirzadi, A.** (2010): A meshless method for two-dimensional diffusion equation with an integral condition. *Eng. Anal. Bound. Elem.*, vol. 34, no. 12, pp. 1031–1037.
- Abbasbandy, S.; Shirzadi, A.** (2011): MLPG method for two-dimensional diffusion equation with Neumann's and non-classical boundary conditions. *Appl. Numer. Math.*, vol. 61, pp. 170–180.
- Ang, W. T.** (2001): A boundary integral equation method for the two-dimensional diffusion equation subject to a non-local condition. *Eng. Anal. Bound. Elem.*, vol. 25, no. 1, pp. 1–6.
- Ang, W. T.** (2008): A dual-reciprocity boundary element approach for solving axisymmetric heat equation subject to specification of energy. *Eng. Anal. Bound. Elem.*, vol. 32, no. 3, pp. 210–215.
- Atluri, S.** (2004): *The meshless method (MLPG) for domain and BIE discretizations*. Tech Science Press.
- Atluri, S.; Shen, S.** (2002): *The Meshless Local Petrov-Galerkin (MLPG) Method*. Tech Science Press.
- Atluri, S.; Zhu, T.** (1998): A new meshless local Petrov-Galerkin (MLPG) approach in computational mechanics. *Comput. Mech.*, vol. 22, no. 2, pp. 117–127.
- Atluri, S.; Zhu, T.** (1998): A new meshless local Petrov-Galerkin (MLPG) approach to nonlinear problems in computer modeling and simulation. *Comput. Modeling Simulation in Engrg.*, vol. 3, pp. 187–196.
- Belytschko, T.; Lu, Y. Y.; Gu, L.** (1994): Element-free Galerkin methods. *Int. J. Numer. Methods Eng.*, vol. 37, no. 2, pp. 229–256.
- Cannon, J.; Lin, Y.** (1990): An inverse problem of finding a parameter in a semi-linear heat equation. *J. Math. Anal. Appl.*, vol. 145, no. 2, pp. 470–484.
- Cannon, J.; van der Hoek, J.** (1986): Diffusion subject to specification of mass. *J. Math. Anal. Appl.*, vol. 115, pp. 517–529.
- Capasso, V.; Kunisch, K.** (1988): A reaction-diffusion system arising in modeling man-environment diseases. *Quart. Appl. Math.*, vol. 46, pp. 431–449.
- Ching, H.-K.; Batra, R. C.** (2001): Determination of crack tip fields in linear elastostatics by the meshless local Petrov-Galerkin (MLPG) method. *CMES: Computer Modeling in Engineering & Sciences*, vol. 2, no. 2, pp. 273–289.
- Dehghan, M.** (2002): Second-order schemes for a boundary value problem with neumann's boundary conditions. *J. Comp. Appl. Math.*, vol. 138, pp. 173–184.

- Dehghan, M.** (2003): Numerical solution of a parabolic equation with non-local boundary specifications. *Appl. Math. Comp.*, vol. 145, no. 1, pp. 185–194.
- Dehghan, M.** (2005): Efficient techniques for the second-order parabolic equation subject to nonlocal specifications. *Appl. Numer. Math.*, vol. 52, no. 1, pp. 39–62.
- Dehghan, M.** (2005): On the solution of an initial-boundary value problem that combines neumann and integral condition for the wave equation. *Numerical Methods for Partial Differential Equations*, vol. 21, pp. 24–40.
- Dehghan, M.** (2006): A computational study of the one-dimensional parabolic equation subject to nonclassical boundary specifications. *Numerical Methods for Partial Differential Equations*, vol. 22, no. 1, pp. 220–257.
- Dehghan, M.** (2007): The one-dimensional heat equation subject to a boundary integral specification. *Chaos, Solitons & Fractals*, vol. 32, no. 2.
- Dehghan, M.; Mirzaei, D.** (2009): Meshless local boundary integral equation (LBIE) method for the unsteady magnetohydrodynamic (MHD) flow in rectangular and circular pipes. *Comput. Phys. Commun.*, vol. 180, no. 9, pp. 1458–1466.
- Dehghan, M.; ShamSi, M.** (2006): Numerical solution of two-dimensional parabolic equation subject to nonstandard boundary specifications using the pseudospectral legendre method. *Numerical Methods for Partial Differential Equations*, vol. 22, pp. 1255–1266.
- Kansa, E. J.** (1986): Application of Hardy’s multiquadric interpolation to hydrodynamics. In *Proc. 1986 Simul. Conf., Vol. 4*, pp. 111–117.
- Ling, L.; Hon, Y. C.** (2005): Improved numerical solver for Kansa’s method based on affine space decomposition. *Eng. Anal. Bound. Elem.*, vol. 29, no. 12, pp. 1077–1085.
- Ling, L.; Schaback, R.** (2008): Stable and convergent unsymmetric meshless collocation methods. *SIAM J. Numer. Anal.*, vol. 46, no. 3, pp. 1097–1115.
- Long, S.; Zhang, Q.** (2002): Analysis of thin plates by the local boundary integral equation (LBIE) method. *Eng. Anal. Bound. Elem.*, vol. 26, no. 8, pp. 707–718.
- Mazzia, A.; Ferronato, M.; Pini, G.; Gambolati, G.** (2007): A comparison of numerical integration rules for the meshless local Petrov-Galerkin method. *Numer. Algorithms*, vol. 45, no. 1-4, pp. 61–74.
- Mirzaei, D.; Dehghan, M.** (2010): Meshless local Petrov-Galerkin (MLPG) approximation to the two dimensional sine-gordon equation. *J. Comp. Appl. Math.*, vol. 233, no. 10, pp. 2737–2754.
- Noye, B.; Dehghan, M.** (1994): Explicit solution of two-dimensional diffusion subject to specification of mass. *Math. Comput. Simulat.*, vol. 37, no. 1, pp. 37–45.

Qian, L. F.; Batra, R. C.; Chen, L. M. (2004): Analysis of cylindrical bending thermoelastic deformations of functionally graded plates by a meshless local Petrov-Galerkin method. *Comput. Mech.*, vol. 33, no. 4, pp. 263–273.

Sellountos, E. J.; Sequeira, A.; Polyzos, D. (2011): A new LBIE method for solving elastodynamic problems. *Eng. Anal. Bound. Elem.*, vol. 35, no. 2, pp. 185–190.

Shirzadi, A.; Ling, L.; Abbasbandy, S. (2012): Meshless simulations of the two-dimensional fractional-time convection-diffusion-reaction equations. *Eng. Anal. Bound. Elem.*, vol. 36, pp. 1522–1527.

Sladek, J.; Sladek, V.; Atluri, S. N. (2000): Local boundary integral equation (LBIE) method for solving problems of elasticity with nonhomogeneous material properties. *Comput. Mech.*, vol. 24, no. 6, pp. 456–462.

Sladek, V.; Sladek, J. (2010): Local integral equations implemented by MLS-approximation and analytical integrations. *Eng. Anal. Bound. Elem.*, vol. 34, no. 11, pp. 904–913.

Sladek, V.; Sladek, J.; Zhang, C. (2010): On increasing computational efficiency of local integral equation method combined with meshless implementations. *CMES: Computer Modeling in Engineering & Sciences*, vol. 63, no. 3, pp. 243–263.

Tulong, Z.; Jindong, Z.; Atluri, S. N. (1999): A meshless numerical method based on the local boundary integral equation (LBIE) to solve linear and non-linear boundary value problems. *Eng. Anal. Bound. Elem.*, vol. 194, no. 6-8, pp. 375–389.

Zhang, Z.; Liew, K.; Cheng, Y.; Lee, Y. (2008): Analyzing 2D fracture problems with the improved element-free Galerkin method. *Eng. Anal. Bound. Elem.*, vol. 32, no. 3, pp. 241–250.

Zhu, T.; Zhang, J.; Atluri, S. N. (1998): A meshless local boundary integral equation (LBIE) method for solving nonlinear problems. *Comput. Mech.*, vol. 22, no. 2, pp. 174–186.

